

Critical edge between frozen extinction and chaotic life

Roberto A. Monetti and Ezequiel V. Albano*

Instituto de Investigaciones Físicoquímicas Teóricas y Aplicadas (INIFTA), Facultad de Ciencias Exactas, Universidad Nacional de La Plata, Sucursal 4, Casilla de Correo 16, (1900) La Plata, Argentina

(Received 18 July 1995)

The cellular automata “game of life” (GL) proposed by J. Conway simulates the dynamic evolution of a society of living organisms. It has been extensively studied in order to understand the emergence of complexity and diversity from a set of local rules. More recently, the capability of GL to self-organize into a critical state has opened an interesting debate. In this work we adopt a different approach: by introducing stochastic rules in the GL it is found that “life” exhibits a very rich critical behavior. Discontinuous (first-order) irreversible phase transitions (IPT’s) between an extinct phase and a steady state supporting life are found. A precise location of the critical edge is achieved by means of an epidemic analysis, which also allows us to determine dynamic critical exponents. Furthermore, by means of a damage spreading study we conclude that the living phase is chaotic. The edge of the frozen-chaotic transition coincides with that of the IPT’s life extinction. Close to the edge, fractal spreading of the damage is observed; however, deep inside the living phase such spreading becomes homogeneous.

PACS number(s): 05.50.+q, 05.40.+j, 64.60.Ht, 05.70.Ln

I. INTRODUCTION

The deterministic cellular automata “game of life” (GL) invented by Conway [1] has been extensively studied. The GL is a two-dimensional lattice system in which the state of each lattice site depends on deterministic local rules. The simple algorithm of the GL simulates the dynamic evolution of a society of living individuals. Processes such as growth, death, survival, self-propagation, and competition are considered. Early studies on the GL have focused on understanding the emergence of complexity and diversity from a few simple local rules [1–5]. More recently, Bak, Chen, and Creutz [6] have proposed that the GL develops into a self-organized critical (SOC) state. These SOC evidences have been questioned by Bennett and Bourzutschky [7] and subsequently an interesting debate has been established [8–10].

In this work we adopt a different approach by introducing stochastic rules in the GL. So the proposed stochastic game of life (SGL), in contrast to Conway’s deterministic GL, may also help us to understand the dynamic evolution of a society in the presence of random noise. The SGL is defined in two dimensions where each lattice site may be in two states, representing the presence or absence of a live individual. The fate of each state depends on the eight nearest neighbors. So the rules for the evolution of the system are as follows: (1) A live individual that has four or more live neighbors will die in the next step (decease by overcrowding). Also, a live site will die in the next step if it has one or zero live neighbors (decease by isolation). However, if the live individual has two or

three live neighbors it will remain alive with probability p_s (survival probability). (2) At a dead site, a new individual will be born at the next time step if it has three live neighbors, however, if the site has two live neighbors an individual will be born only with probability p_b (birth probability).

All births and deaths take place simultaneously. The stochastic components of the model have been selected such as for $p_b=0$ and $p_s=1$ the deterministic Conway GL is recovered.

Starting with a random distribution of live sites, the SGL evolves according to rules (1) and (2) until it reaches a stationary state. The nature of this state solely depends on the stochastic parameters of the model: for some set of values (p_s, p_b) the system evolves toward extinction and the final state is an empty lattice, while for the complementary set of parameters the density of live individuals remains finite. A critical edge is the border between the live and the extinct phases. So the aim of this work is to study the critical behavior of the SGL by means of Monte Carlo numerical simulations. The study is mainly based upon both epidemic and damage spreading analysis. Although the SGL is not related in any obvious way to specific physical or biological systems, there are various considerations that have led us to examine its properties. From the physical point of view we are interested in the nonequilibrium dynamics of the SGL in connection with other far from equilibrium irreversible processes such as, for example, irreversible phase transitions (IPT’s) in catalyzed reaction systems [11,12]. Also, very recently the onset of chaotic behavior within the active phase of the latter processes has been established [13–15], so this possibility is also analyzed within the context of the SGL. From the biological point of view the noise introduced in the present model improves the deterministic GL since biological systems, especially evolu-

*FAX: 0054-21-254642. Electronic address: ealbano@isis.unlp.edu.ar

tionary ones, have a strong factor of indeterminism. This paper is organized as follows: Section II gives brief details of the simulation; in Sec. III the phase diagram is discussed; the theoretical background and results of the epidemic analysis are treated in Sec. IV and Sec. V is devoted to the damage spreading analysis. Finally, our conclusions are stated in Sec. VI.

II. BRIEF DETAILS ON THE SIMULATION

In this paper we study the statistics of relevant aspects of the dynamic critical behavior of the SGL. The system is a two-dimensional square lattice of size L ($100 \leq L \leq 300$) with periodic boundary conditions. The fate of each site depends on the eight neighbors, i.e., the eight sites surrounding the site under consideration, or in other words, the first and second crystallographic nearest neighbors in a two-dimensional square lattice. We started at $t=0$ with a random distribution of living sites with probability ρ_0 . As in standard cellular automata procedures, at each time step all sites are updated simultaneously according to the rules stated in the previous section. It should be noted that the stationary state of the GL model depends on the initial conditions [2]. The asymptotic density of living individuals ρ takes the value $\rho \approx 0.03$ for initial densities in the range $0.15 \leq \rho_0 < 0.75$ [5]. A remarkable feature of SGL is that the stationary state is less sensitive to the initial conditions than in the GL, so all results presented here correspond to $\rho_0=0.5$.

III. THE PHASE DIAGRAM

Starting with a random distribution of live sites with probability $\rho_0=0.50$, the SGL is allowed to evolve according to rules (1) and (2) until it reaches a stationary state. Figure 1 shows, for the steady state, the depend-

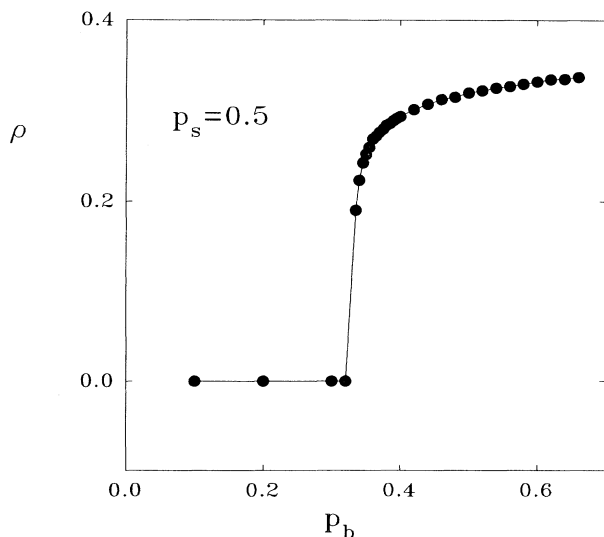


FIG. 1. Plot of the density of live individual ρ vs p_b obtained keeping $p_s=0.50$ constant.

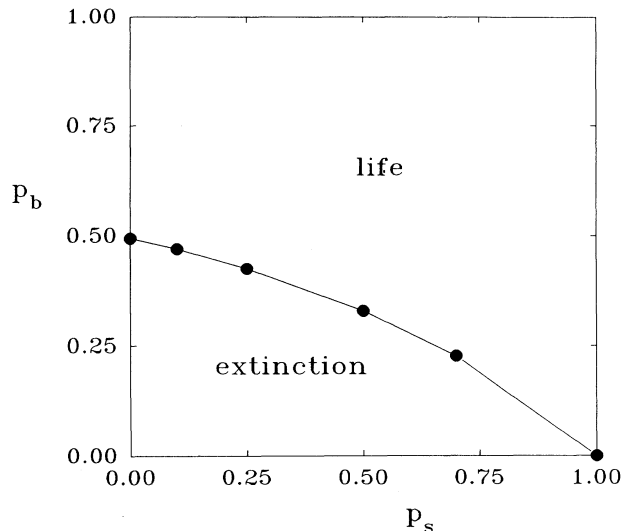


FIG. 2. Plot of the critical points p_b^c vs p_s for the extinction-life edge.

dence of the density of live sites (ρ) on p_b keeping $p_s=0.50$ constant. For small values of p_b , all live sites and their ascendants have died. However, increasing p_b the onset of life is abruptly observed at a certain critical point of coordinates (p_b^c, p_s^c) . The abrupt variation of ρ at criticality indicates the existence of a first-order IPT. Scanning p_b , a set of critical points is obtained, which defines a critical curve $p_b^c(p_s)$, as is shown in Fig. 2. So a critical edge limiting two phases characterized by extinction and life is found. Points in Fig. 2 correspond to critical values determined quite precisely and studied in detail in the forthcoming sections. The critical line has been drawn evaluating critical points from a set of plots of ρ vs p_b , as shown in Fig. 1 and therefore is less accurate. The occurrence of first-order IPT's is a common feature of other irreversible far from equilibrium models describing heterogeneously catalyzed reactions such as the monomer-dimer model [11], the monomer-monomer model [11], the dimer-dimer model [16], the dimer-dimer-monomer model [17], etc. So the understanding of these processes has attracted considerable theoretical effort [18,19].

IV. EPIDEMIC ANALYSIS

A. Theoretical background

It should be stressed that for L finite the steady state of each particular system is metastable because, due to fluctuations of the stochastic processes, there is always a finite probability of life to become extinct. This probability increases when approaching the critical edge, and consequently it becomes difficult to precisely evaluate critical points using a set of plots as in Fig. 1. This shortcoming can be avoided performing an epidemic

analysis [19]. Furthermore, this analysis allows us to determine reliable critical exponents related to the dynamic critical behavior of the system.

The epidemic analysis is performed as follows: one starts, at $t=0$, with a small colony of living sites in an otherwise dead landscape, i.e., a configuration close to the extinct state. Then, the evolution of the colony according to the rules of the SGL is monitored and the following quantities are computed: (i) The average number of live individuals $N(t)$ and (ii) the survival probability of the colony $P(t)$ at time t . Finite-size effects are absent because the system is taken large enough to avoid the presence of live individuals at the boundaries. Averages are taken over 10^4 samples and runs are performed up to $t=1100$.

At criticality, the following scaling behavior holds [19,20]:

$$P(t) \propto t^{-\delta} \quad (1)$$

and

$$N(t) \propto t^{\eta} \quad (2)$$

where δ and η are *dynamic* exponents. At criticality, one expects that log-log plots of $P(t)$ and $N(t)$ vs t would give straight lines, while upward and downward deviations will occur even slightly off criticality. This behavior would allow a precise determination of the critical points and the critical exponents δ and η .

B. Results and discussion

Figure 3 shows a log-log plot of $P(t)$ vs t taken for different values of p_b close to criticality and keeping $p_s = \text{const}$. The asymptotic straight line obtained for $p_b^c = 0.10$ and $p_b^c = 0.470$ is the signature of critical behavior, while slight upward and downward deviations for other p_b values indicate supercritical and subcritical behavior, respectively. The same conclusion follows after analyzing log-log plots of $N(t)$ vs t ; see, e.g., Fig. 4. In all

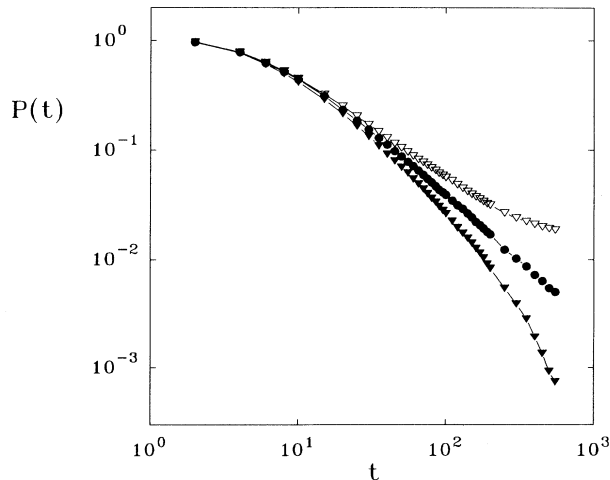


FIG. 3. Log-log plots of $P(t)$ vs t obtained keeping $p_s = 0.10$ constant and taking $p_b = 0.475$ (upper curve), $p_b = 0.47$ (medium curve), and $p_b = 0.465$ (lower curve).

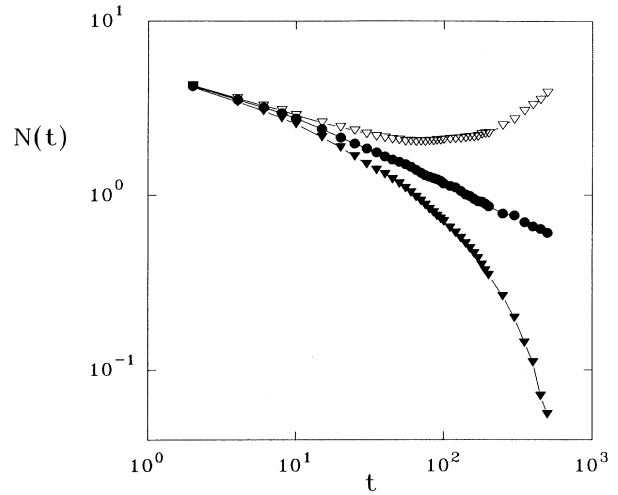


FIG. 4. Log-log plots of $N(t)$ vs t obtained keeping $p_s = 0.10$ constant and taking $p_b = 0.475$ (upper curve), $p_b = 0.47$ (medium curve), and $p_b = 0.465$ (lower curve).

cases the epidemic is started with one glider (i.e., a colony of five live individuals [1]) placed at the center of the sample. Of course, the critical exponents must be independent of the starting colony, as is confirmed in Fig. 5, which shows that the asymptotic slope of log-log plots of $N(t)$ vs t is the same when gliders, blinkers, and ponds [1] are used to initialize the epidemic.

Figures 6(a) and 6(b) show plots of $N(t)$ and $P(t)$ vs t obtained at different critical points. The corresponding critical exponents δ and η , as listed in Table I, are obtained by means of least-square fits of the asymptotic behavior of the corresponding curves. It is observed that when the parameters of the model approach the standard GL limit ($p_s \rightarrow 1$ and $p_b \rightarrow 0$) the asymptotic slopes of the

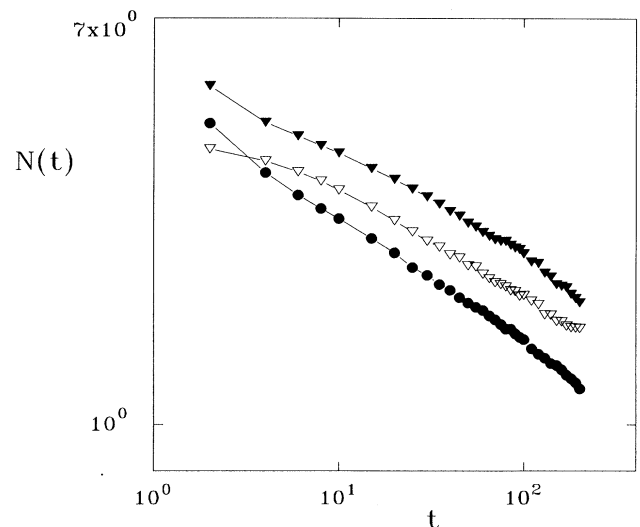


FIG. 5. Log-log plots of $N(t)$ vs t obtained at the critical point $p_s^c = 0.25, p_b^c = 0.425$, and using different initial colonies: ponds (upper curve), blinkers (medium curve), and gliders (lower curve).

TABLE I. Critical points and critical exponents of the SGL. The error bar in parentheses merely reflects the statistical error in the last digit.

p_s	p_b	η	δ
0.0	0.493(2)	-0.264(3)	1.024(7)
0.1	0.470(2)	-0.392(3)	1.180(5)
0.25	0.425(2)	-0.507(2)	1.306(4)
0.5	0.329(2)	-0.268(2)	1.000(5)
0.7	0.227(2)	-0.070(4)	0.790(5)

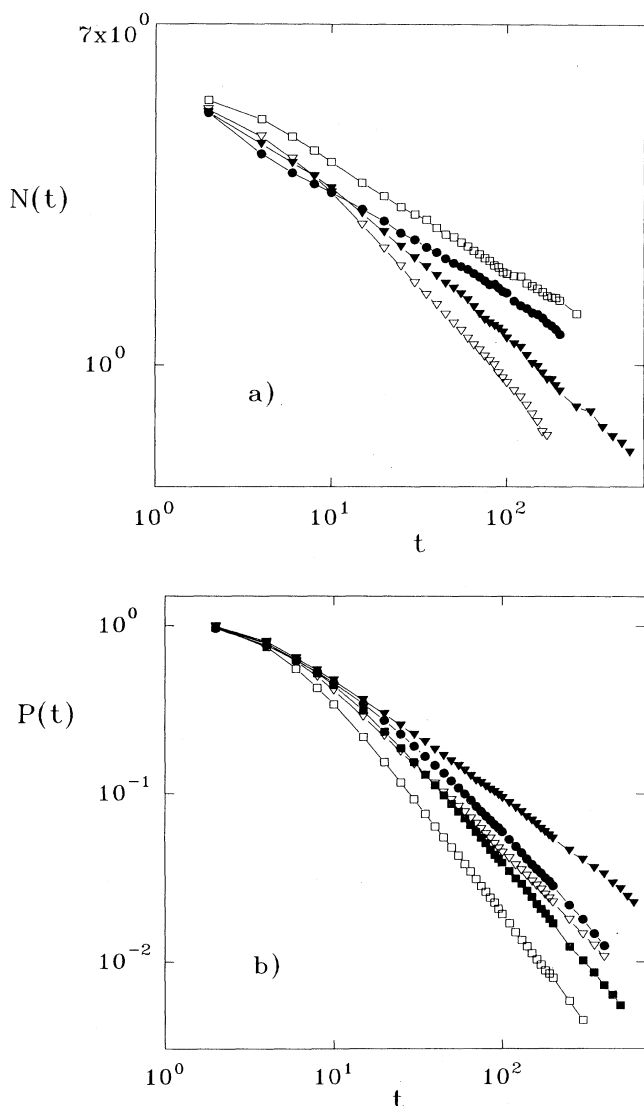


FIG. 6. (a) Log-log plots of $N(t)$ vs t obtained at different critical points: $p_s^c=0.50, p_b^c=0.329$ (\square); $p_s^c=0.0, p_b^c=0.4935$ (\bullet); $p_s^c=0.250, p_b^c=0.425$ (\blacktriangledown); and $p_s^c=0.10, p_b^c=0.47$ (∇). (b) Log-log plots of $P(t)$ vs t obtained at different critical points: $p_s^c=0.70, p_b^c=0.227$ (\blacktriangledown); $p_s^c=0.00, p_b^c=0.4935$ (\bullet); $p_s^c=0.50, p_b^c=0.329$ (∇); $p_s^c=0.250, p_b^c=0.425$ (\blacksquare); and $p_s^c=0.10, p_b^c=0.470$ (\square).

curves shown in Figs. 6(a) and 6(b) approach zero. This behavior is expected since an isolated colony in an otherwise dead sea is stable: it neither reproduces nor dies.

As follows from Table I, the critical exponents obtained at various critical points of the extinction-life edge depend on the critical points. This behavior is due to the fact that the IPT is discontinuous (first order), and therefore long-range correlations capable of absorbing the local details of the model are absent. This is in contrast with second-order IPT's where long-range correlations dominate the critical behavior of the system and consequently universality is observed [20–23]. Furthermore, for first-order (second-order) IPT's the exponent η is negative (positive) [19,24].

V. DAMAGE SPREADING ANALYSIS

A. Theoretical background

The damage spreading problem consists first in taking a steady-state configuration of the SGL σ^A and creating at $t=0$ an initial small perturbation or damage $D(0)$ in that configuration (which gives a second configuration σ^B). Then, one investigates the time evolution of both configurations, using the same dynamic. Such configurations will describe trajectories in the phase space. We want to investigate whether the dynamic of the process is chaotic. The case in which two initially close trajectories quickly become different is generically called chaotic. In order that the concept of closeness of trajectories be meaningful one must have a definition of distance in phase space. A useful metric is given by the Hamming distance or damage, defined by [25]

$$D(t) = (1/M) \sum_{i=1}^M |\sigma_i^A(t) - \sigma_i^B(t)|, \quad (3)$$

where M is the number of sites of the system. So $D(t)$ just measures the fraction of sites for which both configurations are different. Starting with a small $D(0)$ value, $D(t)$ will go asymptotically to zero in the so-called frozen phase, whereas it will tend to a finite value different from zero in the so-called chaotic phase.

While the study of damage spreading in a system exhibiting reversible phase transitions has received much attention (for a review see [25]), only few similar studies in systems undergoing IPT's have been performed [14,15]. These studies reveal the existence of a new and rich dynamic critical behavior.

B. Results and discussion

As in the study of the phase diagram (Sec. III), the square lattice is initialized with a random distribution of live sites with probability $p=0.50$. Then the system is allowed to evolve, according to rules of the SGL, until it reaches a steady state in order to obtain a stationary configuration $\{\sigma^A\}$. If the central site of $\{\sigma^A\}$, with coordinates $(L/2, L/2)$, has two or three live neighbors a damaged configuration $\{\sigma^B\}$ is made. Within the extinct phase all starting configurations evolve toward empty lattices, so one always has $D(\infty)=0$ and the extinct phase

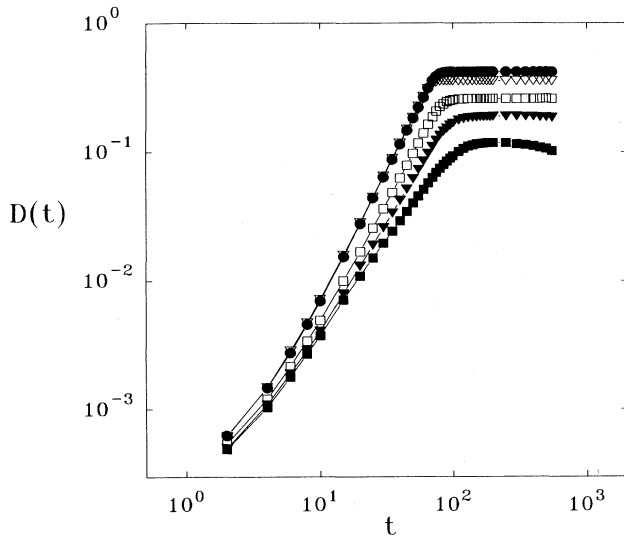


FIG. 7. Log-log plots of $D(t)$ vs t obtained keeping $p_s=0.0$ constant and taking $p_b=1.0$ (\bullet), $p_b=0.6$ (∇), $p_b=0.496$ (\triangledown), $p_b=0.5$ (\square), and $p_b=0.494$ (\blacksquare).

is obviously “frozen.” Figure 7 shows log-log plots of $D(t)$ vs t obtained for different values of p_b keeping $p_s=0.5$ constant. The same behavior is observed for all sets of points within the living phase; i.e., the damage grows almost linearly (in a log-log scale) until it reaches a plateau. Also, the saturation value of the damage decreases when approaching the critical edge. So, we conclude that the living phase is chaotic, and therefore the critical edge of the IPT between life and extinction is the same as that of the frozen-chaotic transition.

Figure 8(a) shows log-log plots of $D(t)$ vs t obtained using lattices of different size L but keeping both $p_s=0.5$

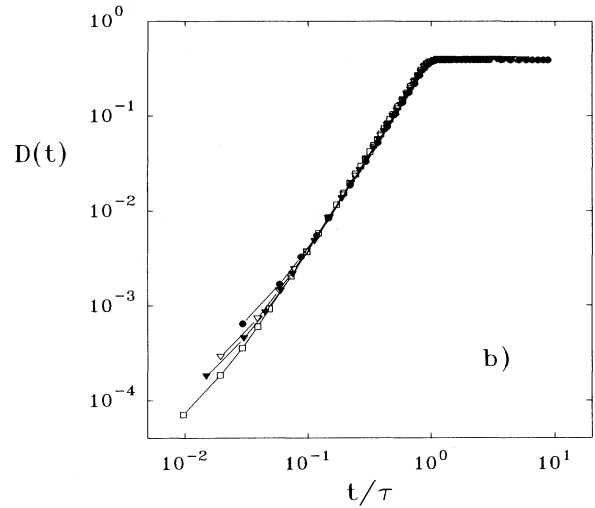
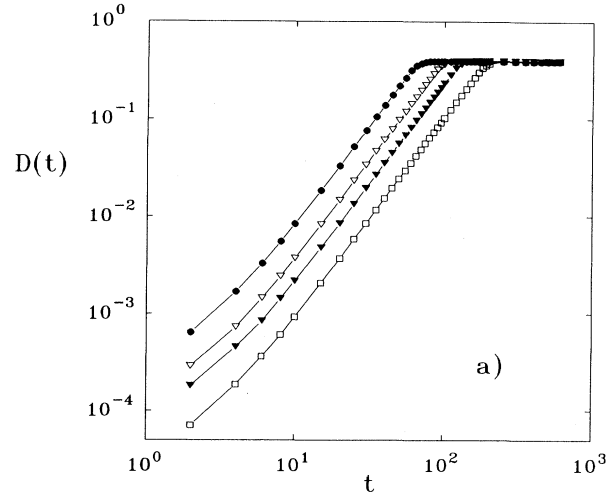


FIG. 8. (a) Log-log plots of $D(t)$ vs t obtained using lattices of different size and keeping both $p_s=0.5$ and $p_b=0.70$ constant. $L=100$ (\bullet), $L=150$ (∇), $L=200$ (\triangledown), and $L=300$ (\square). (b) Log-log plots of $D(t)$ vs t/τ for the data shown in (a).

TABLE II. Values of the exponents α, β, d_f , and the saturation time $\tau(l)$ corresponding to different values of the parameters p_s and p_b . The error bars in parentheses merely reflects the statistical error in the last digit.

p_s	p_r	α	β	d_f	τ
0.0	0.494	1.456(3)	1.631(3)	1.785(5)	109.0 \pm 2.0
0.0	0.496	1.672(3)	1.765(3)	1.895(5)	95.0 \pm 2.0
0.0	0.50	1.839(3)	1.841(3)	1.998(5)	82.0 \pm 2.0
0.0	0.6	2.000(3)	2.000(3)	2.000(5)	70.0 \pm 2.0
0.0	0.8	2.000(3)	2.000(3)	2.000(5)	73.0 \pm 2.0
0.0	1.0	2.000(3)	2.000(3)	2.000(5)	78.0 \pm 2.0
0.25	0.6	2.000(3)	2.000(3)	2.000(5)	69.0 \pm 2.0
0.25	0.8	2.000(3)	2.000(3)	2.000(5)	72.0 \pm 2.0
0.25	0.9	2.000(3)	2.000(3)	2.000(5)	73.0 \pm 2.0
0.25	1.0	2.000(3)	2.000(3)	2.000(5)	75.0 \pm 2.0
0.5	0.35	1.977(3)	1.985(3)	1.992(5)	70.0 \pm 2.0
0.5	0.7	2.000(3)	2.000(5)	2.000(5)	68.0 \pm 2.0

and $p_b=0.70$ constant. It is found that the initial slopes and saturation values of all curves are independent of L . However, the time required for the system to reach the plateau $\tau(L)$ depends on L . It is because the damage propagation velocity is constant, i.e., the larger the lattice size L the longer the time τ required to reach the edges. This behavior suggests that the following scaling ansatz should hold:

$$D(x) \propto \begin{cases} x^\alpha, & x \leq 1, \\ \text{const}, & x > 1, \end{cases} \quad (4)$$

where $x=t/\tau(L)$ and α is an exponent. In fact, Fig. 8(b) shows that excellent data collapsing is obtained using Eq. (4). The obtained values of the exponent α are listed in Table II. It is found that most values are close to $\alpha=2$ but smaller values of α are obtained when approaching the critical edge.

The average square distance $R^2(t)$ over which the initial damage has spread, from the center of the sample towards the boundaries, has also been evaluated. Figure 9 shows plots of $R^2(t)$ vs t obtained for different values of p_b and keeping $p_s=0.0$ constant. It is found that $R^2(t)$ and $D(t)$ exhibit a similar behavior, so the following scaling ansatz should also hold:

$$R^2(x) \propto \begin{cases} x^\beta, & x \leq 1, \\ \text{const}, & x > 1, \end{cases} \quad (5)$$

where β is an exponent (for the result see Table II).

The number of damaged sites is related to the spatial extent of the damage through the fractal dimension (d_f) of the damaged cloud, so

$$D(t) \propto R^{d_f}(t). \quad (6)$$

So, using Eqs. (4) and (5) it follows that

$$2\alpha = \beta d_f. \quad (7)$$

The values of d_f calculated from Eq. (7) are listed in

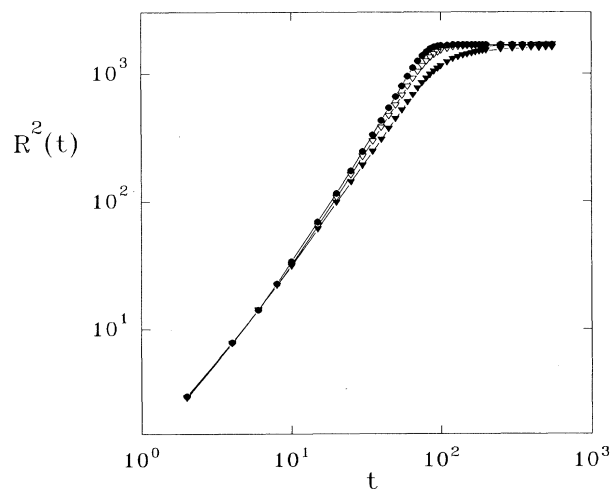


FIG. 9. Log-log plots of $R^2(t)$ vs t obtained keeping $p_s=0.0$ constant and taking $p_b=0.5$ (\bullet), $p_b=0.496$ (∇), and $p_b=0.494$ (\blacktriangledown).

Table II. It is observed that in most cases $d_f=2$. The fractal dimension of the cloud d_f is less than 2 only for values of the parameters very close to the critical edge, where the damaged region is a fractal object. These figures suggest that deep inside the living phase the spreading of the damage is compact and homogeneous. However, when approaching the critical edge and due to the sudden drop in the density of living individuals (see Fig. 1), only fractal spreading can be observed. This behavior becomes evident from the snapshot configurations shown in Fig. 10.

VI. CONCLUSIONS

A Stochastic game of life model is formulated and studied. The stochastic components are introduced to Conway's game of life through two parameters, namely, the surviving and birthing probabilities, p_s and p_b , respectively. The system presents two phases, an extinct phase where the density of living individuals vanishes and a living phase ($0 < \rho < 1$), depending on the parameter values. The abrupt variation of ρ at criticality indicates

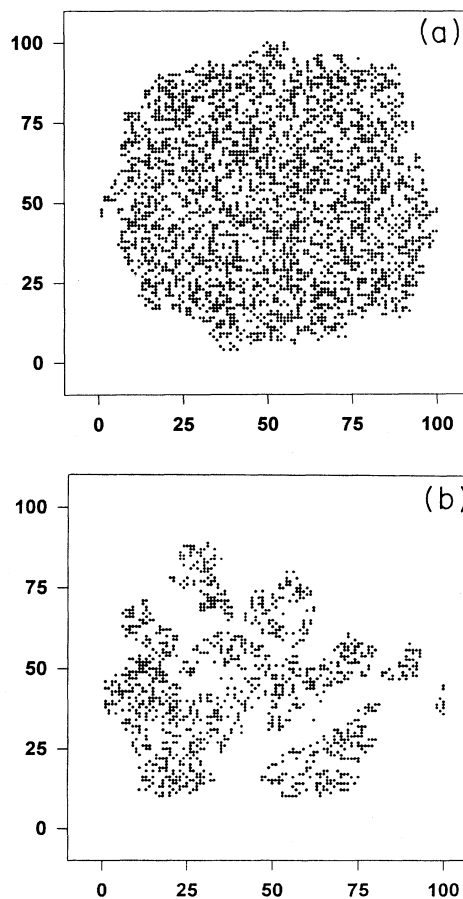


FIG. 10. Typical snapshot configurations showing the damaged cloud, initialized at the center of the sample, just when it reaches one of the edges. Results obtained for $p_s=0.5$ and (a) $p_b=0.70$ (well inside the living phase), and (b) $p_b=0.331$ (close to the critical edge).

the existence of a first-order IPT. The critical points and the same dynamic critical exponents are calculated by means of the epidemic analysis. A damage spreading analysis leads to the conclusion that the living phase is chaotic and the critical edge of the IPT between life and extinction is the same as that of the frozen chaotic transition. Well inside the living phase the cloud of damaged cells is homogeneous, so the spreading of the damage is compact. However, close to the critical edge fractal spreading is found. Of course, the stochastic game of life is not a realistic model for any particular living system. However, it shows a very rich irreversible critical

behavior, also present in actual systems of biophysical interest.

ACKNOWLEDGMENTS

This work was financially supported by the Consejo Nacional de Investigaciones Científicas y Técnicas (CONICET), Argentina. The Volkswagen Foundation (Germany) is greatly acknowledged for the grant of valuable equipment.

-
- [1] E. R. Berlekamp, J. H. Conway, and R. K. Guy, *Winning Ways for your Mathematical Plays* (Academic, New York, 1982), Vol. 2.
 - [2] L. S. Schulman and P. L. Seiden, *J. Stat. Phys.* **19**, 293 (1978).
 - [3] F. Bagnoli, R. Rechtman, and S. Ruffo, *Physica* (Amsterdam) **171A**, 249 (1991).
 - [4] T. R. M. Sales, *Phys. Rev. E* **48**, 2418 (1993); *J. Phys. A* **26**, 6187 (1993).
 - [5] J. B. C. Garcia, M. A. F. Gomes, T. I. Jyh, T. I. Ren, and T. R. M. Sales, *Phys. Rev. E* **48**, 3345 (1993).
 - [6] P. Bak, K. Chen, and M. Creutz, *Nature* **342**, 780 (1989).
 - [7] C. Bennet and M. S. Bourzutschky, *Nature* **350**, 468 (1991).
 - [8] J. Hemmingsson, *Physica D* **80**, 151 (1995).
 - [9] P. Alstrom and J. Leao, *Phys. Rev. E* **49**, R2507 (1994).
 - [10] M. Pacczuski, S. Maslov, and P. Bak, *Europhys. Lett.* **27**, 97 (1994).
 - [11] R. Ziff, E. Gulari, and Y. Barshad, *Phys. Rev. Lett.* **56**, 2553 (1986).
 - [12] E. V. Albano, *Phys. Rev. Lett.* **69**, 656 (1992).
 - [13] K. Fichtorn, E. Gulari, and R. Ziff, *Phys. Rev. Lett.* **63**, 1527 (1989).
 - [14] E. V. Albano, *Phys. Rev. Lett.* **72**, 108 (1994).
 - [15] E. V. Albano, *Phys. Rev. E* **50**, 1129 (1994).
 - [16] E. V. Albano, *J. Phys. A* **25**, 2557 (1992); and *Corrigendum* **26**, 3667 (1993).
 - [17] E. V. Albano, *Surf. Sci.* **306**, 240 (1994).
 - [18] E. V. Albano, *J. Phys. A* **27**, 3751 (1994).
 - [19] J. Evans and M. Miesch, *Phys. Rev. Lett.* **66**, 833 (1991).
 - [20] P. Grassberger and A. De La Torre, *Ann. Phys. (N.Y.)* **122**, 373 (1979); P. Grassberger, *J. Phys. A* **22**, 3673 (1989).
 - [21] I. Jensen, H. C. Fogedby, and R. Dickman, *Phys. Rev. A* **41**, 3411 (1990).
 - [22] I. Jensen, *Phys. Rev. E* **47**, 1 (1993).
 - [23] E. V. Albano, *J. Phys. A* **26**, L881 (1994).
 - [24] J. Evans and T. R. Ray, *Phys. Rev. E* **50**, 4302 (1994).
 - [25] H. J. Herrmann, in *The Monte Carlo Method in Condensed Matter Physics*, edited by K. Binder (Springer-Verlag, Berlin, 1992), Vol. 71.